The Challenges of Measuring Rainfall: Observations Made at the Goodwin Creek Research Watershed

Lisa Sieck, Matthias Steiner, Stephen Burges, James Smith, Carlos Alonso

Abstract

A major storm passing over the 21.4 km^2 Agricultural Research Service (ARS) Goodwin Creek experimental research watershed in northern Mississippi on April 23-24, 2001 is used as a case study to highlight uncertainties associated with using hydrological and hydrometeorological data from various remote-sensing and point sources at greatly differing space-time resolution and coverage. Instrumentation of the research watershed includes approximately 45 rain gauges of various designs (above ground and buried), a raindrop spectrometer, and stacked anemometers to observe the wind profile at the climate station in the center of the catchment. A local-scale mobile Doppler radar was also deployed to record very high-resolution precipitation observations (50 m by 1 degree in space, tens of seconds in time) in both the vertical and horizontal directions over the catchment. These data, along with regional-scale lower-resolution observations from the Memphis WSR-88D (KNQA) radar (1 km by 1 degree in space, several minutes in time), are utilized to analyze the storm. The difficulties of obtaining accurate measurements and of merging observations made by point and remote sources are discussed. The basin response to the storm is illustrated with runoff measurements at the basin outlet.

Keywords: rainfall estimation, uncertainties, radar, rain gauge, drop size distribution

Sieck is a Research Assistant and Burges a Professor, both in the Department Civil and Environmental Engineering, University of Washington, Seattle, WA 98195. E-mail: lsieck@u.washington.edu. Steiner is a Research Scientist and Smith a Professor, both at Princeton University, Princeton, NJ 08544. Alonso is a Hydraulic Engineer/Research Leader, National Sedimentation Laboratory, Oxford, MS 38655.

Introduction

Monitoring the water budget on a catchment requires an accurate representation of rainfall and its variability. Such representations can be used for flood and erosion mitigation. Precipitation is highly variable in space and time, and this variability affects our capability to build a complete picture of rainfall reaching the surface from either in-situ or remote sensing measurements. The lack of continuous observations in space and time requires a merging of information obtained from various point (e.g., rain gauges) and remote sources (e.g., radar) at differing resolution, coverage, and accuracy.

A central issue of the merger of point and remote rainfall information is how much of the observed variance between radar-based estimates and rain gauge measurements can be attributed to sensor resolution differences. For example, both sensors may yield precise measurements at their respective resolution yet the two observations are likely not identical. Detailed observations of rainfall in space and time were thus carried out over the small 21.4 km^2 ARS Goodwin Creek watershed (Figure 1) in northern Mississippi (Alonso 1996, Steiner et al. 1999) to address this question. The instrumentation at this site includes approximately 45 rain gauges of varying design, a Joss-Waldvogel (1967) raindrop spectrometer (often called disdrometer), four anemometers mounted at different heights above the ground to observe the wind profile, and a Surface Radiation (SURFRAD) network station (Hicks et al. 1996) to determine the energy budget located in the center of the catchment (latitude 34° 15' 16" N, longitude 89° 52' 26" W) (Figure 2).

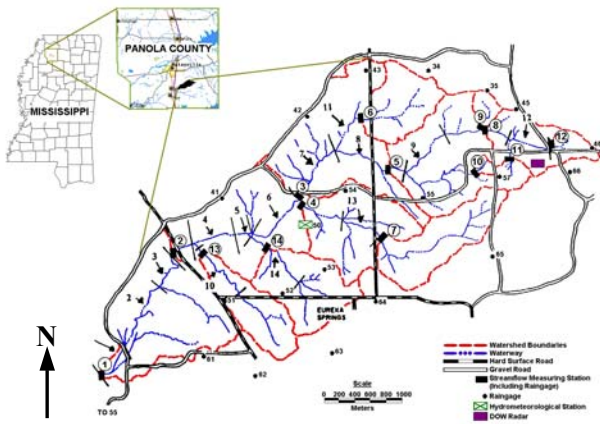A mobile "Doppler-on-Wheels" (DOW) radar system (Figure 3) was used to provide high-resolution storm

Figure 1. Geographical location and instrumental setup of the ARS Goodwin Creek research watershed in northern Mississippi.
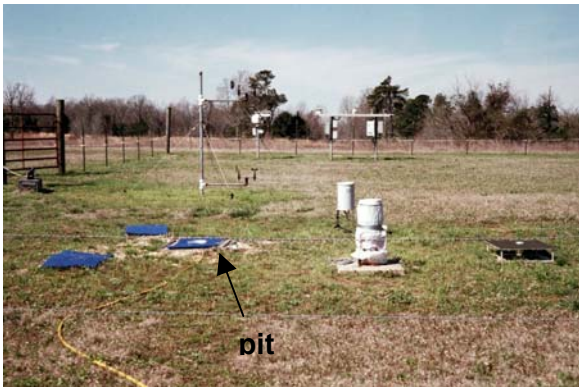

Figure 2. Climatological station (station 50) in the catchment center includes above-ground and buried/pit rain gauges, a disdrometer, wind profile measurements, and a SURFRAD station.

Figure 3. Doppler-on-Wheels (DOW) radar of the University of Oklahoma (deployment site marked by rectangle at upper end of catchment in Figure 1).

intensity and motion observations for several storms passing over the Goodwin Creek area. The DOW operates at a 3 cm wavelength (X band), providing reflectivity and radial velocity data at 50 m by 1 degree resolution in space and updates within tens of

seconds in time (Wurman et al. 1997). The Goodwin Creek watershed is also under coverage from four Weather Surveillance Radar – 1988 Doppler (WSR-88D) radars (Heiss et al. 1990). These radars operate at a 10-cm wavelength (S band) and collect data at a resolution of 1 km by 1 degree in space and several minutes in time. The closest of these WSR-88D (i.e., KNQA) is located near Memphis, Tennessee, approximately 120 km to the north of the Goodwin Creek catchment.

These data are used to characterize and discuss the difficulties of obtaining accurate measurements of rainfall reaching the surface by means of rain gauges and radar. In particular, we evaluate measurement issues associated with the rain gauge catch (e.g., calibration and wind effects) and radar rainfall estimation (e.g., calibration, signal attenuation, and reflectivity to rain rate conversion). Analyses of the 23-24 April 2001 storm illuminate the high variability of rainfall in space and time and limitations of using short-wavelength (X band) radar for hydrologic applications.

Storm Analyses

The storm that crossed Goodwin Creek on April 23-24, 2001 was part of a major storm system that extended from southern Texas to Canada (Figure 4). It was well organized, with an intense line of convection (squall line) followed by some widespread (stratiform) rainfall. The storm passage over Goodwin Creek is reflected in the rainfall trace shown in Figure 5 indicating that there was an initial rainfall shower before the most intense part of the storm. The catchment's response to this rainfall event is shown in the bottom panel of Figure 5. The radar and rain gauge analyses are discussed in following sections.
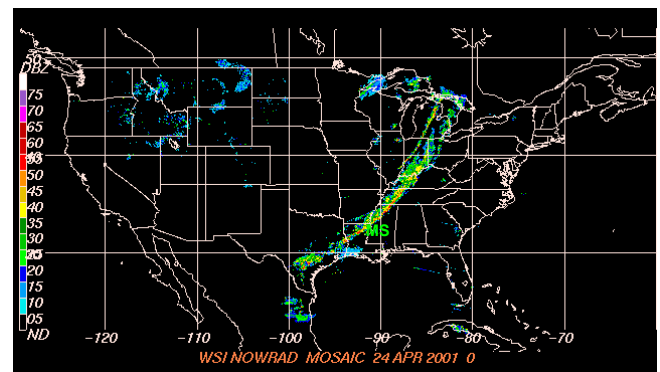

Figure 4. Weather Services International radar reflectivity mosaic of storm on 23-24 April 2001 at 0000 UTC as it passes over Northern Mississippi.
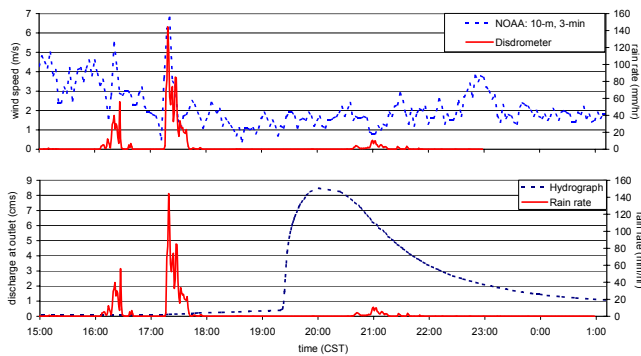
199

Figure 5. The top panel shows the 10-m wind speed (dashed) plotted with rain rate from disdrometer (solid) in the center of catchment (station 50). The discharge at the outlet of Goodwin Creek (station 1) is shown in the bottom panel.

Radar analysis

Figures 6 through 9 reveal key aspects of the storm as seen by the local DOW and remote Memphis KNQA radars. Figure 6 shows a horizontal snapshot of the storm on April 23, 2001, 2201 UTC. The left and right panels show the reflectivity observations made by the DOW deployed at the eastern end of the watershed (see Figure 1) and the KNQA radars, respectively. The KNQA reflectivity is shown only for the area covered by the DOW. The KNQA data have been adjusted in time to minimize the root-mean-square difference between DOW and KNQA observations.
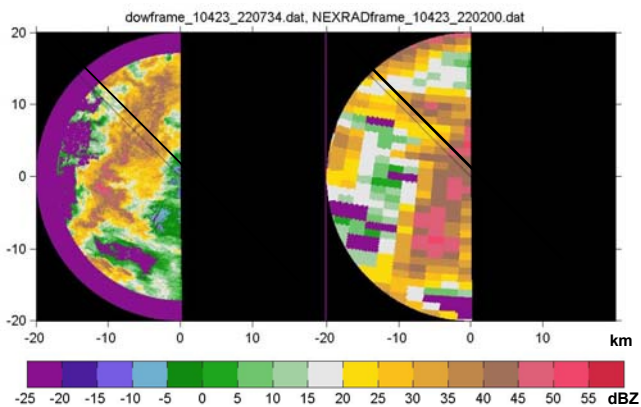

Figure 6. Horizontal cross-section of storm reflectivity as seen by the DOW at 2207 UTC (left) and the KNQA at 2202 UTC (right) radar on April 23, 2001. The dark line denotes the 315° azimuth.

The DOW provides an order of magnitude increase in spatial resolution over the KNQA radar. At this finer resolution, significant small-scale structures within the convective line can be seen that are not resolved

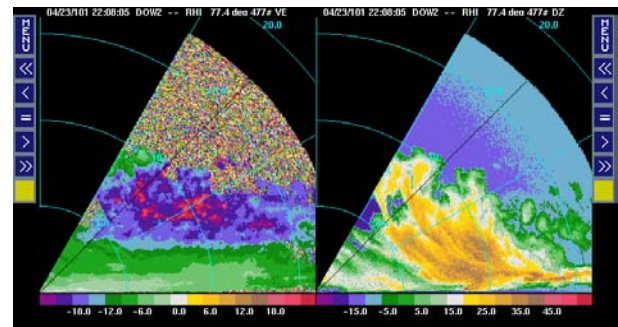by the KNQA. This is especially true for the vertical structure shown in Figure 7.

Figure 7. Vertical cross-section of radar radial Doppler velocity (left panel) and reflectivity (right panel) as observed by the DOW radar on April 23, 2001 at 2208 UTC. Range rings are shown at 5 km intervals.

Figure 8 shows a snapshot of the storm on April 23, 2001 at 2319 UTC as seen by the DOW and the KNQA radars during the passage of the most intense part of the storm when rain rates reached 150 mm/h. The vertical cross-section (Figure 9) illustrates how the air is lifted up along the frontal boundary (left panel) and precipitation formed, yet this cross section also demonstrates the severe limitation of radar reflectivity observations made at shorter wavelengths – a complete loss of signal in radial direction behind the intense convective cell (right panel). This attenuation effect can also be seen in the horizontal depiction of the storm by comparing the DOW and KNQA reflectivities in Figure 8.
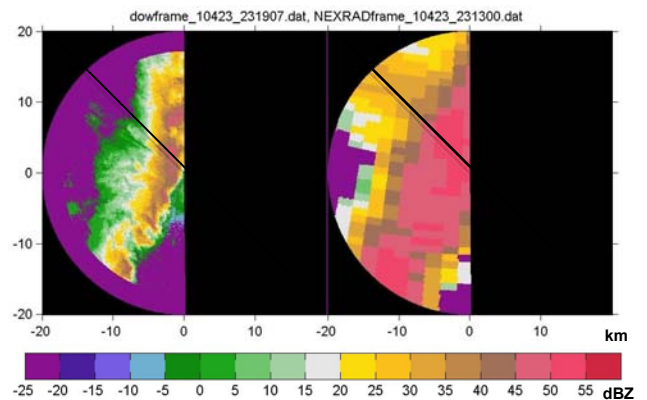

Figure 8. Horizontal cross-section of storm reflectivity as seen by the DOW at 2319 UTC (left) and the KNQA at 2313 UTC (right) radar on 23 April 2001. The dark line denotes the 315° azimuth.
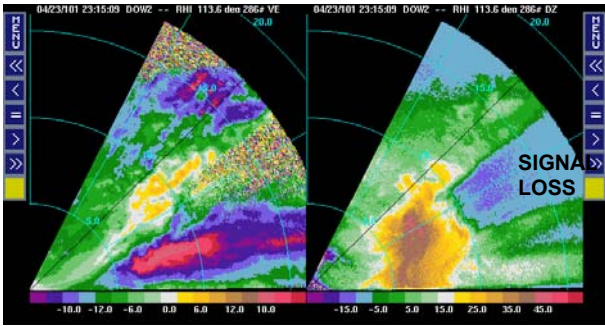
Figure 9. Vertical cross-section of radar radial Doppler velocity (left panel) and reflectivity (right panel) as observed by the DOW radar on April 23, 2001 at 2315 UTC.

The earlier snapshots (Figures 6 and 7) do not reveal an attenuation problem even though the rain rates were also high (approximately 80 mm/h). The difference in attenuation between the two time periods may be explained by the fact that the second and more intense rainfall period was associated with a significant amount of lightning, indicating that this part of the storm included high-density ice particles such as graupel or small hail that cause a different behavior of the radar signal.

Figure 10 shows a time series of reflectivity calculated based on the raindrop spectra at the center of the Goodwin Creek catchment compared to the closest reflectivity pixels observed by both the DOW and KNQA radars. The radar-based intensities nicely trace the observed rainfall at the surface considering the significant differences in sampling volume and sampling frequency. The attenuation problem of the DOW observations can be clearly seen for the passage of the most intense part of the storm (after 2300 UTC). Signal attenuation is less evident during the first rainfall burst (2200 – 2230 UTC).
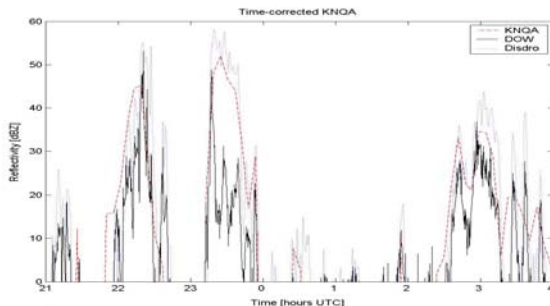

Figure 10. Reflectivity based on disdrometer observations at station 50 and closest pixel of DOW and KNQA radar.

The loss of DOW signal can be estimated with respect to the KNQA observations by comparing DOW and KNQA reflectivities along a common path, and (safely) assuming that the KNQA (S-band) observations are not attenuated. Attempts to quantify the loss of DOW signal in this manner, however, are complicated by the spatial and temporal resolution differences between the KNQA and the DOW – there are approximately 400 DOW pixels that correspond to a single KNQA pixel at any given location and there are more than 20 DOW sweeps in time for each KNQA radar sweep. Figure 11 shows such a comparison along the DOW azimuth 315° (see Figure 8). Note the rapid decrease of DOW signal with distance from the radar, as well as the significant variability with time. DOW signals within 2 km of the radar (vertical line, Figure 11) were not considered for this analysis because of a questionable close-range correction.
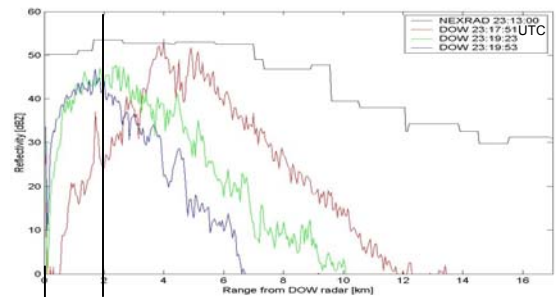

Figure 11. Reflectivity vs. distance from the DOW for both the time corrected KNQA and DOW radar.

Iterative attenuation corrections, constrained by the KNQA and raindrop spectra-derived reflectivities, have not been successful for the most intense storm front, possibly because of the added complexity of high-density ice particles contained in the DOW radar sampling volume. Moreover, this correction procedure depends on the radar calibration. In order to achieve a reasonable calibration, the KNQA and DOW radar reflectivities have been compared to the raindrop spectra based values for weak to moderate rainfall, where the X-band attenuation for the DOW observations should be small.

Point rainfall analysis

The ultimate test of successful data quality control and correction is to compare the radar-estimated rainfall amounts to rain gauge-based surface measurements. The Goodwin Creek rain gauge network consists of several different types of instruments, including Belfort weighing gauges (BEL), Texas Instruments tipping bucket gauges (TXI), USDA Agricultural Research Service tipping

bucket gauges (ARS), Australian Hydrologic Service tipping bucket gauges (TB3), and simple buried/pit collectors (COL) that have their rim at ground level (see Figure 2). At least one of each type of gauge was operated at the climatological station in the center of the catchment during this storm. Also, one tipping bucket gauge was mounted above ground (sARS) while another by the same manufacturer was buried (bARS).

The collected water in the BEL gauges was measured after the storm to compare with the amount recorded on the chart. Moreover, water collection devices have been installed for some of the ARS and TXI tipping bucket gauges and the TB3, providing an independent measure of rainfall for these gauges. Detailed calibration curves have been established for most gauges to correct for rain rate dependent effects. Pit collectors (COL) were buried next to several of the gauges to obtain a best estimate of the "true" rainfall reaching the surface.

The rainfall information collected for the 23-24 April 2001 storm passing over the Goodwin Creek watershed is compiled in Table 1. The instruments worked properly, with the exception of a few rain gauges (5, 6, and 62) and one disdrometer (DIS2). Although the calibration for two of the Belfort weighing rain gauges (50 and 57) was somewhat questionable, this gauge type was the most reliable. This is due to its sturdy design and built-in capability for redundant measurements (i.e., chart recording of weighed rain amount, plus collection of total water). The tipping bucket gauges were more prone to malfunction. In addition, the calibration of the ARS gauges varied by as much as ± 10%. The TXI gauges were more stable but one still varied by + 10%. The water from TXI gauges 41, 43, 46 and 65 was collected to check against the cumulative quantity indicated by the gauge tips. Volume collection checks were also made for ARS gauges at stations 1 and 50 (surface and buried). The collection of the water flowing through the ARS and TXI gauges was difficult and, indeed, this check system did not work reliably at gauge 43 for this storm. However, the agreement of collected water amounts with the tip-based rain totals was encouraging. Even for a well-maintained network, rain gauges are prone to malfunctioning, demonstrating the need for multiple gauges at a "point" location to enable cross-checking of values to reveal data inconsistencies.

Table 1. Rainfall accumulations (mm) measured by gauges across the catchment using manufacturer (Mcal) or individual (Ical) gauge calibrations and estimated by the KNQA and DOW radars at the gauge locations. Collected values are shown as well (Collect).

No	Type	MCal	Ical	Collect	KNQA	DOW
1	ARS	22.6	23.4	23.4	27	3.82
1	COL			24.2	27	3.82
2	ARS	23.6	23.1		24.1	4.59
4	ARS	25.4	26.8		24.5	5.45
5	ARS	0.76	0.79		30.8	4.37
6	ARS	3	3.2		31.3	4.86
7	ARS	24.9	27.4		26.2	2.92
8	ARS	30.7	34.2		27.9	3.67
11	ARS	25.1	27.9		30.2	2.70
12	ARS	24.4	22.2		30.2	
13	ARS	26.7	28.4		24.1	4.25
14	ARS	26.1	26.6		24.3	5.02
34	BEL	26.2	-	30.7	31.8	5.31
35	BEL	29.2	-	31	27.9	3.77
41	TXI	23.4	25.6	24.3	24.1	3.69
41	COL			26.2	24.1	3.69
42	TXI	25.4	27.3		31.7	4.88
43	TXI	26.9	28.4	21.6	34.1	4.07
43	COL			29.6	34.1	4.07
45	TXI	26.7	29.3		24.8	1.93
46	TXI	26.2	28.2	27.4	28	
46	COL			27.1	28	
50	sARS	26.2	25	25.1	24.5	4.97
50	bARS	26.9	30	30.5	24.5	4.97
50	TB3	25.2	24.2	26.1	24.5	4.97
50	COL1			26.6	24.5	4.97
50	COL2			27.1	24.5	4.97
50	DIS1	28.4	-		24.5	4.97
50	DIS2	-	-		24.5	4.97
50	BEL	23.9	-	26.7	24.5	4.97
51	BEL	25.1	-	25.1	20.3	3.95
51	COL			25.5	20.3	3.95
52	TXI	24.4	26.4		21.1	4.30
53	BEL	25.1	-	25.1	21.1	2.41
54	BEL	25.1	-	26.9	30.8	4.24
55	TXI	24.4	26.3		33.1	3.82
57	BEL	22.6	-	26.9	31.9	3.07
57	COL			27.1	31.9	3.07
61	BEL	21.6	-	23.1	22.6	3.57
62	TXI	2.5	2.7		22.4	2.53
63	TXI	23.9	25.5		22.2	3.86
64	BEL	24.9	-	25.9	22.9	4.34
64	COL			26.8	22.9	4.34
65	TXI	25.1	27.3	25.7	28.6	2.76
66	BEL	26.7	-	26.7	28	

Another potentially significant source of uncertainty for rain gauge measurements is wind effects on the catch. The wind may come in strong gusts, often associated with the most intense parts of storms (see Figure 5), which makes it difficult to assess quantitatively. For our purposes, we estimated the wind effect on the rain gauge catch by comparing the rainfall amounts of the above-ground to the buried gauges. The undercatch due to wind effect estimated this way ranged from 1%-9% depending on location. Whenever possible, it is recommended that rain gauges be buried to reduce the wind effect.
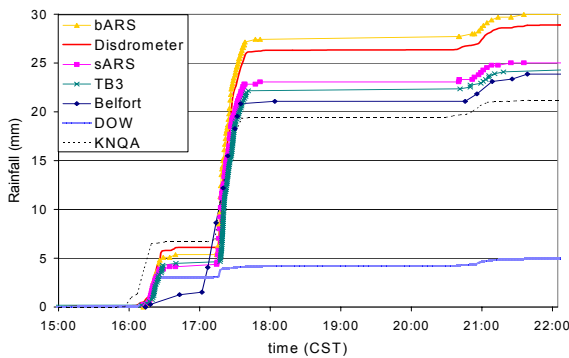

Figure 12. Accumulated rainfall in the center of the Goodwin Creek catchment.
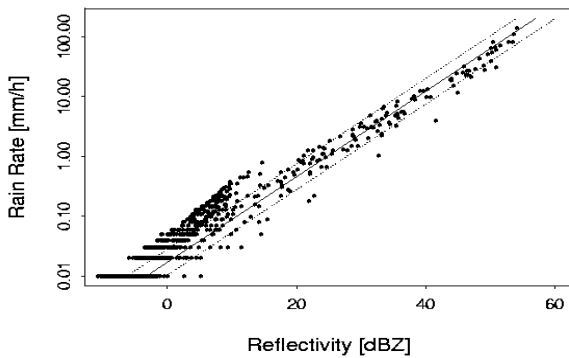

Figure 13. Variability of raindrop size distributions and reflectivity-rain rate relationship for the storm of April 23-24, 2001. Solid line shows a Z-R relationship ($Z = AR^b$) with multiplicative factor A = 300 and power factor b = 1.4, while dotted lines show relationships with A = 600 and A = 150, respectively.

The rainfall accumulations recorded in the center of the watershed are shown in Figure 12. There is significant variation in accumulated rainfall amounts among the various rain gauges, the disdrometer, and the two radars. The 20% variability of accumulated rainfall among the gauges and disdrometer reflects differences in collection mechanisms and wind effects. The radar rainfall estimates shown in Figure

12 and Table 1 are based on the relationship $Z = 300R^{1.4}$ which provides a good fit to the data (Figure 13) based on the raindrop spectra collected in the center of the watershed. While the KNQA radar provides reasonable rainfall amounts, Figure 12 demonstrates the effect of signal attenuation on accumulated rainfall estimates based on the DOW radar. The DOW rainfall estimates amount to less than 20% of the total rain that reached the surface during this storm.

Conclusions

Detailed observations of a major storm system that passed over the small well instrumented ARS Goodwin Creek research watershed in northern Mississippi were used to highlight the range of uncertainty encountered in measuring rainfall from in-situ to remote sensing perspectives. These uncertainties are related to the rain gauge measurements (e.g., calibration, wind effect), radar rainfall estimation (calibration, attenuation, Z-R conversion), and the merging of information from various sources (space and time differences in sampling and coverage). The most accurate spatial rainfall estimates are achieved by combining information from all available data sources.

It is crucial to use only reliable rain gauge information for storm analysis. Rain gauges, especially tipping-bucket gauges, are prone to malfunction. Redundancy is the key to obtaining high-quality rain gauge data. Clusters of at least three rain gauges within tens of meters (or less) are preferable over networks of individual evenly spaced gauges. Clustering allows for cross-checking of data to detect malfunctioning gauges. In addition, rain gauges should be buried if possible to minimize wind effects on the catch.

Mobile short-wavelength radar are increasingly being deployed for rainfall monitoring over urbanizing areas and small catchments. Our study demonstrates, however, that the problem of signal attenuation may seriously limit the quantitative use of such radar for rainfall estimation, especially for situations of intense rainfall that might cause flooding. A correction of radar signal attenuation proves difficult even when additional information is available to constrain an iterative correction procedure.

Analyses of several storms observed in a similar fashion over Goodwin Creek will provide guidance with regard to effectively merging information from various sources to yield the best rainfall measurements. This may include rain gauge and corrected short-wavelength radar observations.

Acknowledgments

References

Alonso, C.V. 1996. Hydrologic research on the USDA Goodwin Creek Experimental Watershed, northern Mississippi. Proceedings of the 16th Annual AGU Hydrology Days Conference, Fort Collins, CO, pp. 25-36. American Geophysical Union.

Heiss, W.H., D.L. McGrew, and D. Sirmans. 1990. NEXRAD: Next Generation Weather Radar (WSR-88D). Microwave Journal 33:79-98.

Hicks, B.B., J.J. DeLuisi, and D.R. Matt. 1996. The NOAA integral surface irradiance study (ISIS): A new surface radiation monitoring program. Bulletin of the American Meteorological Society 77:2857-2864.

Joss, J., and A. Waldvogel. 1967. Ein Spektrograph fuer Niederschlagstropfen mit automatischer Auswertung. Pure and Applied Geophysics 68:240-246.

Steiner, M., J.A. Smith, S.J. Burges, C.V. Alonso, and R.W. Darden. 1999. Effect of bias adjustment and rain gauge data quality control on radar rainfall estimation. Water Resources Research 35:2487-2503.

Wurman, J., J. Straka, E. Rasmussen, M. Randall, and A. Zahrai. 1997. Design and deployment of a portable, pencil-beam, pulsed, 3-cm Doppler radar. Journal of Atmospheric & Oceanic Technology 14:1502-1512.